

Laser-Induced Action Potential-Like Measurements of Cardiomyocytes on Microelectrode Arrays for Increased Predictivity of Safety Pharmacology

Jasmin Schaefer¹, Timm Danker¹, Karin Gebhardt¹, Udo Kraushaar¹

¹NMI Natural and Medical Sciences Institute at the University of Tübingen, Germany,

Corresponding Author

Udo Kraushaar

udo.kraushaar@nmi.de

Citation

Schaefer, J., Danker, T., Gebhardt, K., Kraushaar, U. Laser-Induced Action Potential-Like Measurements of Cardiomyocytes on Microelectrode Arrays for Increased Predictivity of Safety Pharmacology. *J. Vis. Exp.* (187), e64355, doi:10.3791/64355 (2022).

Date Published

September 13, 2022

DOI

10.3791/64355

URL

jove.com/video/64355

Abstract

Life-threatening drug-induced cardiac arrhythmia is often preceded by prolonged cardiac action potentials (AP), commonly accompanied by small proarrhythmic membrane potential fluctuations. The shape and time course of the repolarizing fraction of the AP can be pivotal for the presence or absence of arrhythmia.

Microelectrode arrays (MEA) allow easy access to cardiotoxic compound effects *via* extracellular field potentials (FP). Although a powerful and well-established tool in research and cardiac safety pharmacology, the FP waveform does not allow to infer the original AP shape due to the extracellular recording principle and the resulting intrinsic alternating current (AC) filtering.

A novel device, described here, can repetitively open the membrane of cardiomyocytes cultivated on top of the MEA electrodes at multiple cultivation time points, using a highly focused nanosecond laser beam. The laser poration results in transforming the electrophysiological signal from FP to intracellular-like APs (laser-induced AP, liAP) and enables the recording of transcellular voltage deflections. This intracellular access allows a better description of the AP shape and a better and more sensitive classification of proarrhythmic potentials than regular MEA recordings. This system is a revolutionary extension to the existing electrophysiological methods, permitting accurate evaluation of cardiotoxic effect with all advantages of MEA-based recordings (easy, acute, and chronic experiments, signal propagation analysis, etc.).

Introduction

The electrical contribution of a heartbeat results from a complex and precisely timed interplay of many cardiac channels and transporters, as well as the precisely tuned

propagation of electrical signals through the myocardium¹. Alteration of these closely coordinated mechanisms (e.g., using drugs) can result in severe consequences for the

function of the heart (i.e., life-threatening arrhythmia)^{2,3}. Arrhythmias are defined as irregular heartbeats that alter the normal rhythm of the heart, which can have life-threatening consequences. They may be caused either by impaired initiation of a wave of cardiac excitation or by abnormal propagation of cardiac excitation⁴, which in turn results in a dysfunction of the heart's pumping mechanism.

Many highly potent drug candidates must be excluded from further investigations during the early drug development phase due to their (pro-) arrhythmic potential^{2,3}. They modulate key cardiac channels (e.g., the human ether-a-go-go-related gene channel [hERG]) that are responsible for normal cardiac action potential formation and termination as well as subsequent signal propagation⁵.

Pharmaceutical companies routinely use patch-clamp measurements or microelectrode arrays (MEA) to investigate potential cardiotoxic off-target effects induced by drug candidates. Patch-clamp recordings allow to decipher the impact of substances on cardiac ion channels and to analyze the transcellular cardiac action potential with high spatio-temporal resolution^{6,7}. However, disadvantages of this technique include low throughput with manual patch-clamp and limited applicability of automation due to the dependence of this method on cells in suspension. Furthermore, chronic effects cannot be investigated due to the invasiveness of the method. Finally, typically only single cells are studied simultaneously rather than the entire cardiac syncytium, making it impossible to address information about signal propagation.

Voltage-sensitive dyes are valuable for noninvasively investigating cardiac action potentials and drug-induced arrhythmias⁸. They allow the investigation of both single-cell and syncytium activity. Drawbacks of this method

are cytotoxic effects of either the dyes per se or of the reaction product during illumination. They are used for acute experiments and are hardly applicable for long-term studies^{9,10,11}. Voltage-sensitive proteins as alternatives have made significant progress over the last couple of years in terms of usability and sensitivity but require genetic modification of the cells of interest and lack high temporal resolution compared to electrophysiological techniques¹².

Information from the most recent CiPA initiative¹³ states that MEAs are widely used in cardiac safety screenings as an alternative electrophysiological approach as they represent a powerful and well-established tool to investigate cardiac function and safety pharmacology. Cardiomyocytes are cultivated as a syncytium directly on top of the chips, and extracellular field potentials (FPs) are recorded noninvasively *via* substrate-integrated microelectrodes. This recording principle allows conducting increased throughput screenings over several days, which makes them suitable for pharmaceutical research on chronic effects. The resulting FP waveform is a derivative of the intracellular AP¹⁴. Parameters such as beat rate, the amplitude of the initial part of the FP, and FP duration are easily accessible¹⁵. Other essential criteria such as the differentiation between prolongation and triangulation of the FP (an important marker of proarrhythmia^{16,17}) are inaccessible due to the AC filtering effect of the technique. Furthermore, detecting other small proarrhythmic events such as early and delayed afterdepolarizations (EAD and DAD, respectively) are often easily overlooked due to their small amplitude.

Here we describe a method for gaining access to the intracellular membrane potential by opening the membrane of cardiomyocytes. The IntraCell device (hereafter referred to as intracellular recording device) allows repeated membrane

openings of cardiomyocytes cultivated on top of the MEA electrodes using a highly focused nanosecond laser beam *via* a specific physical phenomenon (surface plasmon resonance)¹⁸. As a result, the recording transitions from a regular FP into an intracellular-like AP (laser-induced AP, liAP). The protocol shows how this allows gaining access to kinetic aspects of the waveform that cannot easily be captured by analyzing FPs. This method represents a bridge between traditional intracellular patch-clamp and MEA recordings. The technology is therefore a powerful extension of current cardiac safety assessment methods.

Protocol

1. Induced pluripotent stem cell-derived cardiomyocytes preparation

NOTE: iCell cardiomyocytes² (referred to as induced pluripotent stem cell [iPSCs]-derived cardiomyocytes) were prepared according to the protocol provided by the supplier. The protocol will be briefly summarized in the following section.

1. Thaw plating and maintenance medium at 4 °C for 24 h prior to use.
 2. Prepare fibronectin coating by dissolving sterile fibronectin in sterile water at a concentration of 1 mg/mL. Freeze store this stock in aliquots (e.g., 25 µL per aliquot). Dilute the aliquoted stock solution 1:20 in sterile Dulbecco's balanced salt solution (dPBS).
 3. Coat the electrode fields of the previously autoclaved MEAs under the laminar flow hood, droplet-wise under sterile conditions with fibronectin using a 10 µL pipette. For this, drop 5 µL of the fibronectin coating solution onto the electrode fields and observe the formation of a droplet on top of the electrode area. Make sure not to touch the sensitive electrodes.
- NOTE:** To maintain sterile conditions, transfer the MEA chip into a sterile Petri dish before removing it from the laminar flow hood.
4. Incubate the coated MEAs for 1 h at 37 °C in an incubator preferably.
 5. Thaw the cryovial containing the cardiomyocytes in a water bath at approximately 37 °C for 2 min until only a little ice crystal is left. Transfer the cell solution gently to a 50 mL tube.
 6. Add 1 mL of plating medium to the empty cryovial. Transfer the solution dropwise over a time period of 90 s into the 50 mL tube to reduce the osmotic shock. Gently add additional 8 mL of plating medium into the tube.
 7. Mix the cell suspension carefully using a 10 mL pipette. Calculate the total number of viable cells using automated fluorescence cytometry. The number should be close to the number in the datasheet provided by the manufacturer.
 8. Spin the cell solution down for 3 min at 200 x g at room temperature. Remove the supernatant by aspiration using a glass pipette attached to a pumping system. Adjust the cell number between 6,000 and 15,000 viable cells/µL.
- NOTE:** The number of cells is usually in the range given above but can vary depending on the respective supplier.
9. Remove the coating solution that was applied in step 1.3 from the MEA electrode area using a 10 µL pipette directly before cell seeding. Seed the cells immediately after the removal to avoid drying of the coating. For this, seed the cells dropwise at 4 µL for both 6-well MEAs and

1-well MEAs onto the electrode fields in the same manner as done with the coating.

10. Allow the cells to adhere for 1 h in the incubator at 37 °C and 5% CO₂ prior to filling the wells with the sterile plating medium heated to approximately 37 °C at 200 µL for 6-well MEA and 1 mL for single well MEA under the laminar flow hood.
11. Perform a complete medium change 48 h after plating under the laminar flow hood. For this, remove the plating medium by aspiration using a glass pipette attached to a pumping system. Then, add 200 µL of sterile maintenance medium heated to 37 °C to the wells.
12. Perform complete medium changes every other day.
13. Start measuring the cells 5-8 days after thawing. Perform a complete medium change 2 h prior to starting the experiments.

2. MEA recordings

NOTE: The device used to transform the FP signal to liAP consists of an upright microscope and a 1064 nm laser.

1. Place the MEA system on top of the device with the MEA chip holder centered over the objective hole. Position the MEA set up so that the objective is directly under the hole of the MEA system to allow the laser to focus on the electrodes.
2. Transfer the MEA chip with the cultivated cells from the incubator to the MEA setup 15 min prior to recording, allowing the cells to recover from the mechanical disturbance.
3. Clean the contact pads and pins carefully using isopropanol and a cotton swab to decrease noise levels. Place the MEA carefully in the MEA-setup. Position the

MEA chip with the logo at the bottom on the top left side (6-well MEA) or with the reference electrode to the left (single-well MEA).

4. Set the MEA system-integrated heating to 38 °C. Place a small chamber on top of the MEA chip to constantly perfuse the cells with humidified carbogen (5% CO₂ and 95% O₂) to recreate incubator conditions and prevent evaporation.
5. Close the lid of the device. The integrated safety switch only allows the laser to be activated if the lid is closed over the MEA chip. Set the MEA system filter using the MEA config program to 0.1 Hz or less high-pass and 3,500 Hz low-pass.
6. Use the MC_Rack software (recording software) or any alternative software for recording. Adjust the input range according to your needs ensuring that the signal does not saturate the amplifier and the sampling rate (e.g., 20 kHz). Use the long-term display function of the software to check the recording.

3. Laser-induced cell poration

1. After inserting the MEA chip into the MEA setup and setting up the software, initialize the laser mechanics using the FB Alps software (initialization software).
2. First, click on the **Initialization** button. At the end of initialization, the virtual laser point will be in well D for a 6-well MEA and at the bottom left for a single-well MEA, respectively.
3. Move the virtual laser point with Ctrl + mouse click into the middle of electrode D5 and adjust the focus. Adjust the focus by Ctrl + scrolling with the mouse wheel.

4. Press the button **Set P1**. The virtual laser point will automatically move into well F. Repeat the process with the electrode F5 and select **Set P2**.
 5. After this procedure, the laser point will move into well B. Repeat the same process with electrode B5 and press **Set P3** in the software. The system is now aligned.
 6. Adjust the laser power and process time according to the needs of your cells. Here, 40% power and 25% process time were used.
 7. To enable the laser, click on the **Laser Off** button, which will then appear as laser on. Switch to the recording software, choose a filename, and click on the **Red Recording** button followed by the **Play** button on top of the window to record the measurement.
 8. Record a baseline of 60 s prior to opening the cells with the laser. Switch back to the initialization software.
 9. Deactivate electrodes to be excluded by the laser on the virtual map on the right-side using Ctrl + mouse click. Select the electrodes of interest by activating them on the array representation on the right-hand side of the software window.
 10. To start the laser, use Alt + mouse click and select the center electrode of this well. This initiates the laser to automatically open the cells on each electrode of this well. Repeat for each well. The laser will then open all the previously activated electrodes of the selected well automatically.
2. Dissolve Nifedipine, E4031, and Dofetilide first in DMSO in mM concentration, and then further in medium to 10x of the desired concentration. Never exceed a final DMSO concentration of 0.1% in the well.
 3. Record the baseline activity for 60 s. Start the laser-induced poration as described in step 3 of the protocol, resulting in a transformation of the FP into liAP shape.
 4. Apply all the drugs as single-concentration-per-well. Remove 20 μ L of medium per well for 6-well MEAs and 100 μ L for single-well MEAs, respectively. Add 20 μ L or 100 μ L, depending on the MEA type, of the stock solution of the drug to be measured to the well and carefully pipette up and down 2-3 times. Perform at least three replications of each drug and concentration to achieve statistical relevance.
 5. Allow the compounds to wash in for 300 s. During this time, the liAP shape may transform back into FP shape. Again, induce laser-induced poration and record possible compound-induced effects on the liAP for an additional 60 s.

5. Data export

4. Drug handling and application

1. Prepare all substances to be used for drug tests freshly on the day of the measurements. Ensure that the final application concentration is 10 times higher in medium to make a 1:10 dilution in the wells.
1. Select relevant electrodes by replaying the recording in the recording software. Use MC_DataTool to convert MC_Rack files to ASCII .txt files.
2. Click on **File > Open MCD > Select a MC_Rack file**. Click on the **txt** button (blue text).
3. Select an electrode. The selected electrode will be shown in the list on the right side.
4. Click on **Browse** to select the folder and change the name of the new .txt file. Click on **Save**.

5. Unselect the exported electrode and select the next electrode to export. Repeat the procedure for all electrodes of interest.

6. Data handling and statistical analysis

1. Import converted binary traces into R¹⁹. Visualize/analyze the data using custom-tailored scripts containing the following packages: dplyr, tidyr, and ggplot2^{20,21,22}.

Representative Results

The recording system used to record electrical activity from cultivated cardiomyocytes consisted of a standard MEA system equipped with a heater and a chamber for carbogen attached to a computer. The system was set on top of the intracellular recording device, which in turn was mounted on top of a small anti-vibration unit (**Figure 1A-B**).

iPSC-derived *cardiomyocytes*² started beating spontaneously within 2-3 days after thawing (days *in vitro*, DIV) and were visible under a microscope. From DIV 4 onward, the beating frequency became regular, and extracellular field potentials (FP) with peak-to-peak amplitudes of the depolarizing component between 1 to 5 mV could be detected on most of the electrodes within the respective wells of the MEA chips. The electrical activity could be detected in more than 95% of the wells under investigation. From DIV 7 onward, the probability of cell detachment increased, making further use of these wells impossible.

The software to control the laser-induced membrane opening allows adjusting both the power and process time of the laser that mediates the opening of the cell membrane only on the electrode under investigation (**Figure 1C**), whereas other electrodes in the respective well are unaffected. While

too conservative settings did not change the waveform of the FP, too high settings resulted in the putative injury of the cardiomyocytes, indicated by vigorous but transient beating or loss of the signal. When adjusted to a setting of 40% power and 25% process time well-tolerated by the cells, triggering of the laser pulse resulted in multiple changes to the recorded waveform (see **Figure 1D** for an exemplary recording). Under these conditions, no alteration of the electrode material was macroscopically observed. The recorded signal amplitude massively increased by 4.1 ± 0.41 (n = 20, range 1.34-8.83) times, analyzed from a randomly picked subset of recordings, resulting in amplitudes between 7 and 22 mV. Furthermore, the waveform transformed from a standard FP shape with rapid, biphasic, and transient voltage deflection at the beginning, followed by a plateau phase back at baseline and a small deflection indicating the end of the FP to a shape that was closer to an intracellularly recorded AP with a rapid rise, extended depolarized plateau phase and a repolarization phase with an undershoot below the baseline (**Figure 1E**). We defined these voltage deflections as laser-induced AP (liAP). In most cases, the transition was transient and at least partially inverted within 5 min. Signal propagation within the cardiac syncytium remained unaltered after liAP induction (**Figure 2**), indicating that the remaining syncytium was not affected by potential damage from the laser pulse.

Similarities to intracellularly recorded APs allowed for extracting parameters of the liAP that are not accessible to FPs (for exemplary parameters see e.g., **Figure 3A**), most prominently the measurement of the duration of the liAP at specific time points (e.g., at 20%, 50%, and 90%) (**Figure 3B**), analogous to APD20/50/90 commonly used for the description of APs.

We next tested the response of the laser-opened cardiomyocytes to commonly used cardioactive pharmacological tool compounds. An exemplary protocol design can be found in **Figure 3C**. Since the transformation of the liAP did not always persist throughout the entire experiment, the compound application was performed as a single-concentration-per-well rather than in a cumulative manner to reduce the total recording time. Nevertheless, it was necessary to either reopen the cells or open another electrode area prior to applying the test compound.

The addition of the specific L-type Ca^{2+} channel blocker, Nifedipine^{23,24}, reduced the plateau phase of the liAP in a concentration-dependent manner and thereby shortened the entire liAP (**Figure 4A,B**). This shortening was comparable to the analysis obtained from FPs of cardiomyocytes from unmanipulated electrodes (**Figure 4C**), indicating that this recording method did not have adverse effects compared to classical FP recordings.

E4031 inhibits the repolarization of relevant Kv1.11 (hERG) potassium channel²⁵ and leads to arrhythmic behavior of cardiomyocytes at increased concentrations. Similar to the analysis obtained from FP recordings, E4031 increased the liAP duration in a concentration-dependent manner (**Figure 5**). Additionally, at concentrations of 0.01 μM and higher, small positive voltage deflections at the end of the liAP were visible. These deflections became more prominent with higher concentrations, indicating a transient new depolarization, unlike in the FPs, where these deflections were virtually invisible (see **Figure 5B-C**, upper (FP) vs lower (liAP) traces). This behavior is known as early afterdepolarization (EAD). At the highest concentration of 0.1 μM , these EADs escalated over time into ectopic beats,

which are premature action potentials (**Figure 5C**). Both EAD and ectopic beats are key indicators of proarrhythmic activity. At the end of the example shown in **Figure 5D**, the electrical activity resulted in arrhythmic beating. Also, concentration-response-relationships displayed between FP and liAP recordings were matching (**Figure 5E**). However, there is more considerable variability in the FP data resulting from the weak repolarization component of the FPs at higher concentrations of the test compound. It seems to be the characteristic nature of iPSC-derived cardiomyocytes² to tend to generate unphysiologically long APs under control conditions also (AP durations > 700 ms). The MEA system applied an intrinsic 0.1 Hz AC filtering, which in turn resulted in a partially filtered shape of the liAP, although without occluding the qualitative information about the onset and termination of the underlying AP.

It turned out that the initial occurrence of proarrhythmic voltage deflections could be detected at lower concentrations in liAPs in comparison to FP recordings. Shown in **Figure 6** is the recording of electrical activity during the application of Dofetilide at a concentration of 3 μM . The recording was obtained in the same well. Although both FP and liAP displayed durations of approximately 2 s, the FP waveform was unobtrusive, presenting regular repolarizing deflections. At the same time, at the end of liAPs, EADs at different magnitudes became visible. This increase in relevant safety-pharmacological sensitivity further supports the finding that liAPs induced by surface plasmon resonance allow improved qualification of the repolarizing phase and thereby help to learn more about the mode of action of the test compounds under investigation.

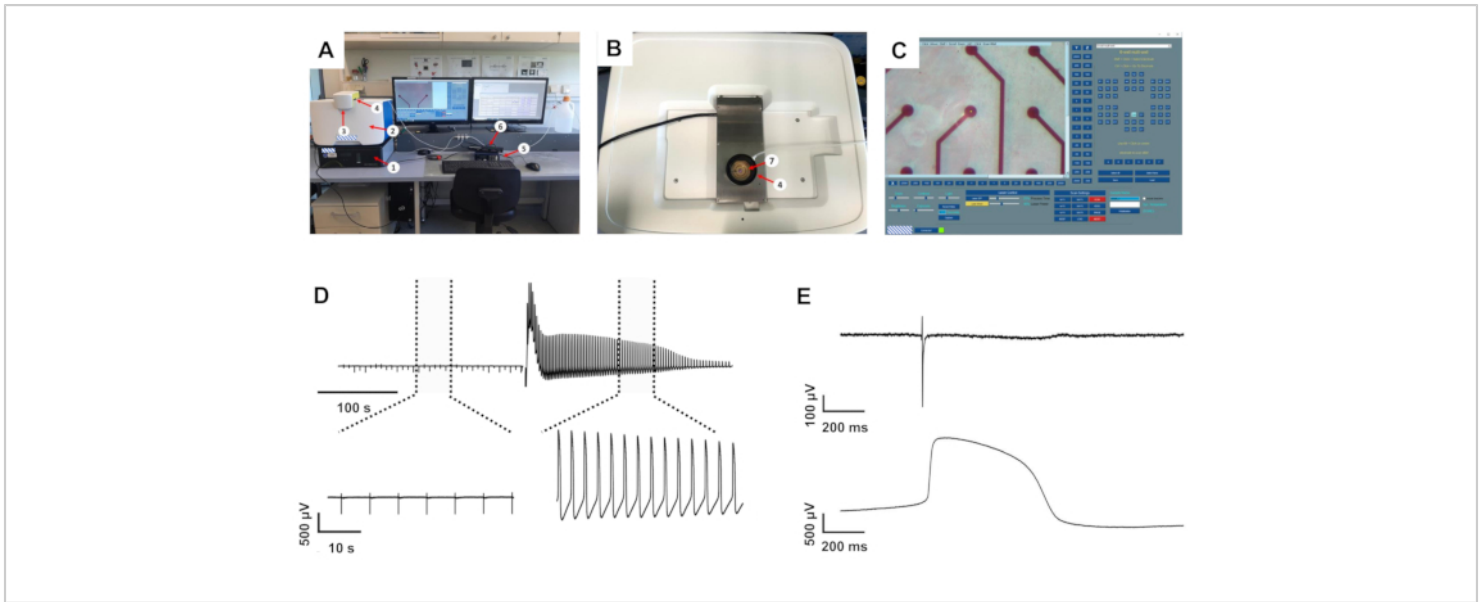


Figure 1: The intracellular recording setup and exemplary recordings. (A) Setup overview. (B) Top view of the recording system with open MEA recording amplifier. (C) Initialization software with the virtual MEA map on the right-hand side. 1: anti-vibration table, 2: intracellular recording system, 3: laser protection lid, 4: humidified carbogen chamber, 5: MEA heating system, 6: MEA interface board, 7: 1-well MEA chip inside the recording amplifier. (D) Recording examples from one electrode before and after induction of liAPs. Top: recording of approximately 6 min. Dotted lines mark the expanded areas shown at the bottom. (E) Magnified FP (top) and liAP (bottom). [Please click here to view a larger version of this figure.](#)

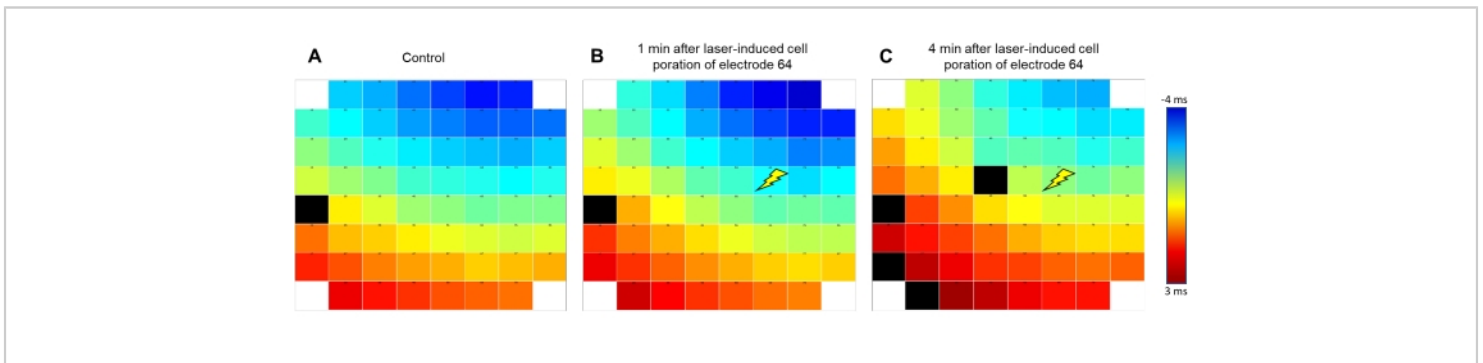


Figure 2: Signal propagation pattern remains conserved after liAP induction. False-color coding of the signal propagation of the excitation wave within the syncytium. Blue indicates early (starting at -4 ms); red indicates late time points (+3 ms) from the signal obtained at reference electrode E54 as indicated by the color bar. The signal travels from top right to bottom left of the electrode array. (A) Before liAP induction, (B) 1 min after liAP induction. (C) 4 min after liAP induction. The Flash symbol indicates the laser induction point at electrode 64. Note that no difference in the overall propagation direction is visible. Black rectangles indicate invalid data. [Please click here to view a larger version of this figure.](#)

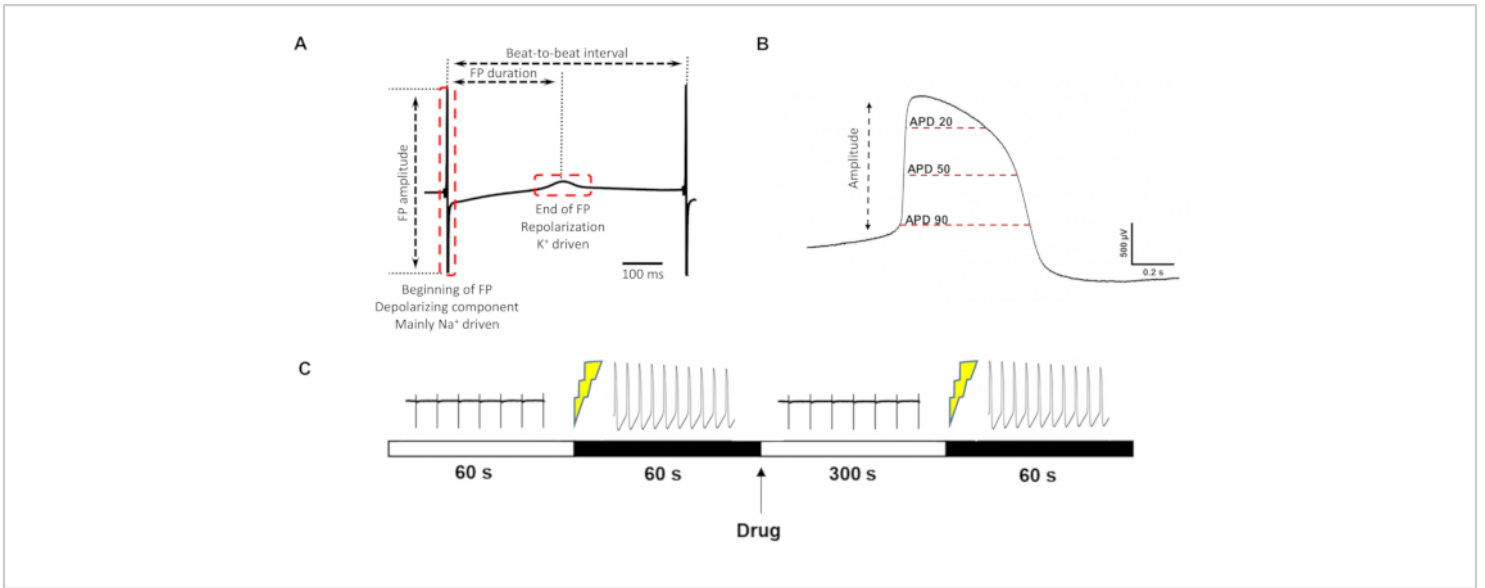


Figure 3: FP/liAP parameter definition and recording protocol. (A) Parameters that can be extracted from the classical FP. **(B)** Additional parameters that can be obtained from liAPs. **(C)** Timeline of drug measurement. From left to right: control recording for 60 s, induction of liAP, recording of liAP for 60 s, drug application, wash-in time 300 s, re-induction of liAP, recording of liAP for 60 s. [Please click here to view a larger version of this figure.](#)

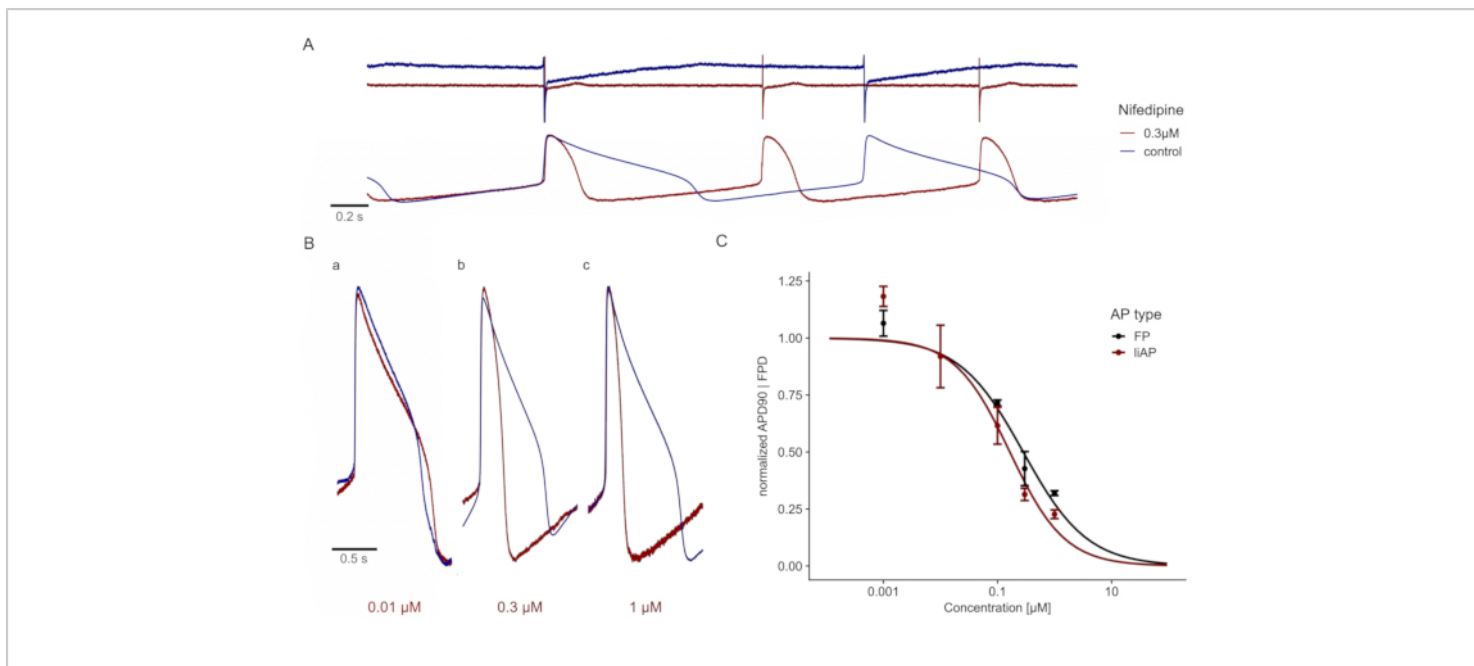


Figure 4: Nifedipine shortens the cardiac liAP in a concentration-dependent manner. (A) Top: FP traces at control (blue) and in the presence of 0.3 μM Nifedipine (red). Traces are displayed with a y-axis offset for better visualization. Bottom: liAP traces from the same MEA recording, resulting in a shortening of the liAP combined with an increase in the beat rate. **(B)** Superposition of single liAPs during control (blue) and application of different concentrations of Nifedipine (red). a: 0.01 μM , b: 0.1 μM , and c: 0.3 μM . Note the shortening of the liAP duration with increasing concentrations. **(C)** The concentration-response relationship of signal width obtained from FP (black) and liAP (red) recordings. Data is from $n = 3$ experiments and normalized to control. Error bars indicate the standard error of the mean. [Please click here to view a larger version of this figure.](#)

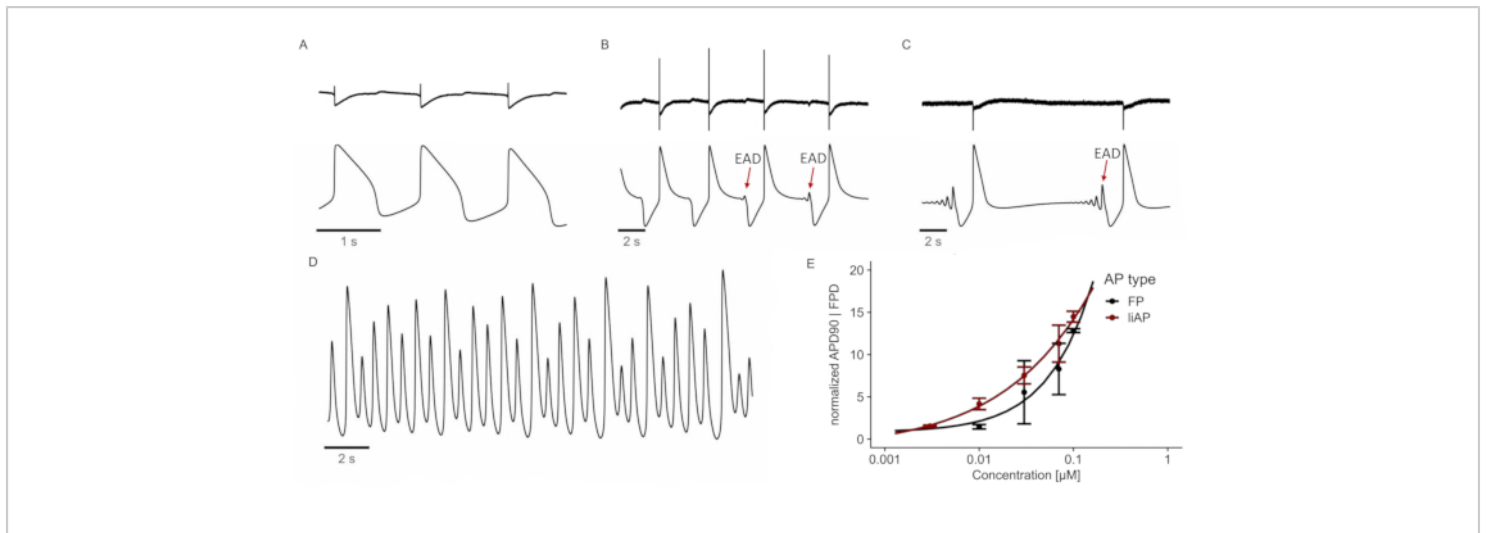


Figure 5: E4031 induces (pro-) arrhythmic behavior. (A) FP (top) and liAP (bottom) at control conditions. **(B-C)** FPs and liAPs were recorded at different time points after applying E4031 (0.1 μM). After 80 s, the first EADs are visible at the end of the liAP (B; marked by a red arrow). EADs convert into ectopic beats after 320 s in the presence of the test compound (C). **(D)** After 530 s, the cardiac syncytium enters a tachycardic state. Trace depicted from liAP recording. **(E)** Concentration-response relationship of FP (black) and liAP (red) width. Data from n = 4 experiments, normalized to control. Error bars indicate the standard error of the mean. [Please click here to view a larger version of this figure.](#)

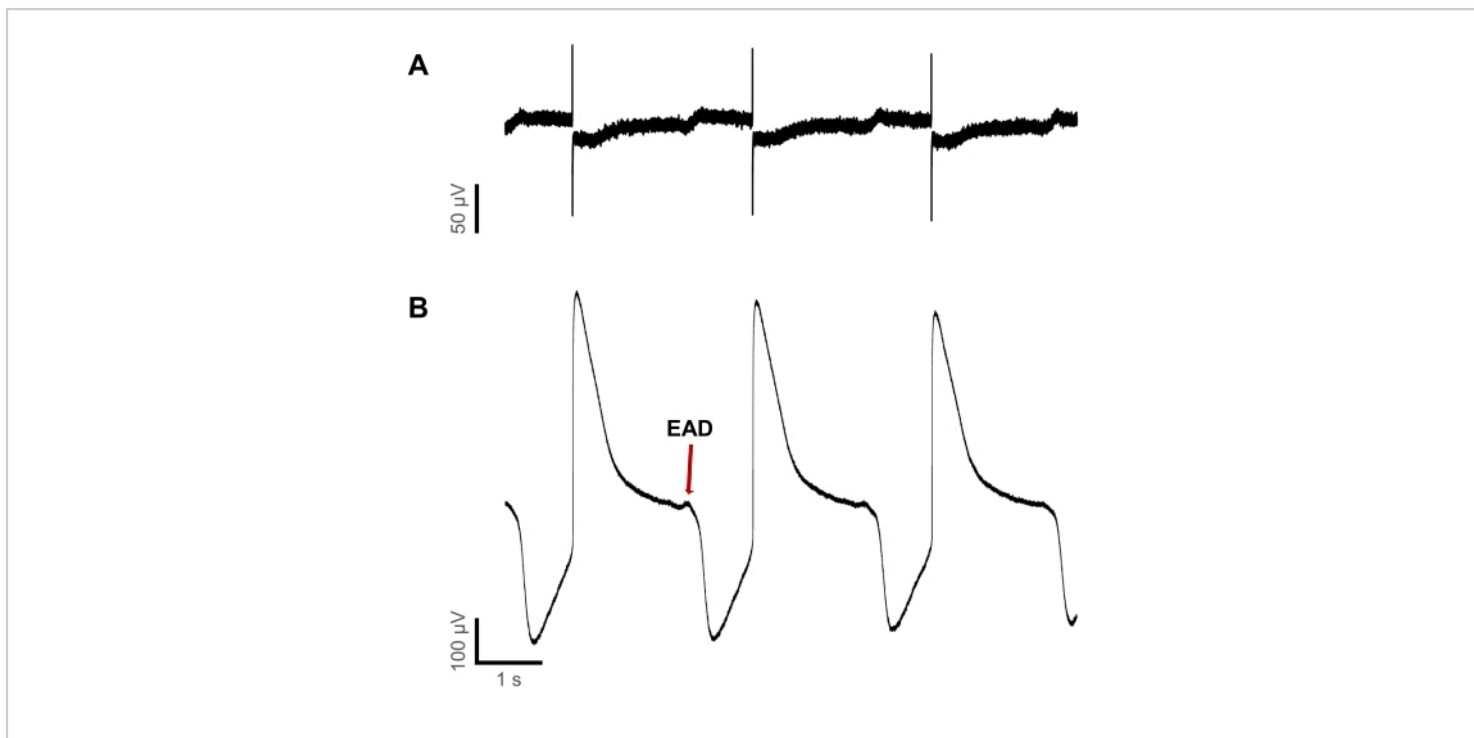


Figure 6: Detection of proarrhythmic events is more sensitive in liAPs than FPs. (A) FP recording and (B) liAP recording within the same well during application of 3 µM Dofetilide. While at the end of some liAPs, EADs are detectable, they remain undiscoverable in FP recordings. [Please click here to view a larger version of this figure.](#)

Discussion

This innovative method demonstrates a new way to investigate *in vitro* the pharmacological modulation of the cardiac action potential during the application of cardioactive pharmacological tool compounds.

Classical MEA recordings allow FP recordings, which are the derivative of the cardiac AP¹⁴. This indirect recording convolves the time course of the de- and repolarization and thereby eliminates essential characteristics of the AP. Furthermore, although the transcellular voltage change of an AP typically reaches values of approximately 100 mV, the overall FP amplitude remains comparably low, with peak amplitudes between several 100 µV and low single-digit mV values. Due to the recording principle, the repolarizing phase

is small; in many cases, it is merely detectable and often of unclear shape, making it difficult to define the end of the FP. The opening of the cell membrane allows us to gain access to the intracellular voltage, thereby uncovering the time course of the cardiac AP. There are multiple advantages of this recording method in comparison to FP recordings. Firstly, the signal amplitude is more prominent, providing a superior signal-to-noise ratio. Secondly, the waveform results in better detection of the repolarization. Thirdly, the shape of the repolarization phase contributes insights into the mode of action of the test compound, provided by the steepness of the signal relaxation. And lastly, this method offers an improved sensitivity to detect critical adverse drug effects,

demonstrated by the recording example displayed in **Figure 6** for the occurrence of EADs in the liAP but not in the FP.

So far, there are two ways of gaining access to the intracellular AP. The first one is achieved by electroporation^{26,27}. Here, short and strong voltage pulses applied *via* the recording electrodes can open the cell membrane²⁸. The second possibility is the membrane opening *via* a laser pulse, making use of a physical phenomenon named surface plasmon resonance, as demonstrated here. One of the advantages compared to electroporation is the increased likelihood of consecutive openings. Due to the highly focused laser spot (1-3 μm) this effect is very locally limited to the electrode of interest. Interestingly, the initiation of the liAP did not alter the signal propagation of the cultivated syncytium. This indicates that, although the cell integrity is damaged, the cardiomyocytes do not seem to depolarize *via* the hole in the membrane.

There are limitations to this method. Like with electroporation, the membrane opening does, in most cases, not last over the entire experimental course. The minimal power and duration settings of the laser pulse required for stable opening of the specific cell type of interest need to be defined independently prior to the experiments. We found (not shown) that the parameters drastically vary between different cell types (in our case, several hiPS-derived and primary cardiomyocytes). This avoids unnecessary stress on the cells during the compound test experiment and results in more reliable and reproducible data. It is of critical importance to adjust the z-axis to provide a clear focus on the cells and the electrodes. An unfocused camera picture yields in a laser spot located at a suboptimal level, potentially resulting in the inability to open the cell membrane. Even with best-adjusted parameters, the liAP effect is transient, and the amplitude reduces over time.

Furthermore, the access to the intracellular space of the cells varies between liAP inductions, both within consecutive openings at the same electrode and between electrodes. This results in high variability of the liAP amplitude. The reason is not yet fully understood. Possible explanations include mechanical issues such as a drift of the laser focus or different subcellular localization of the membrane opening. This makes the analysis of amplitude effects of test compounds complicated at this point in time. Also, recording electrical activity by a MEA system requires high pass filtering to compensate for unavoidable baseline drift. Although in the system used here, this filtering was set to 0.1 Hz (the lowest filter setting available for this system), filtering effects during the plateau phase were still visible, resulting in a slow trend of the voltage deflection toward the baseline during the plateau phase of the cardiac AP. This is especially problematic with extensively long underlying APs like the iPSC-derived iCell cardiomyocytes² used here, which already generate AP >700 ms under control conditions. The use of systems with lower filtering may better conserve the shape of the AP and allow even better access to the time course of the repolarization phase.

Disclosures

The authors have nothing to disclose.

Acknowledgments

The authors would like to thank Foresee Biosystems for lending the IntraCell system during the studies. They would also like to thank Hae In Chang for technical assistance. This work has received funding from the European Union's Horizon 2020's research and innovation program under the grant agreement no. 964518 (ToxFree), from the EU Horizon Europe European Innovation Council Programme, project

SiMulTox (grant agreement No 101057769), and from the State Ministry of Baden-Wuerttemberg for Economic Affairs, Labour and Tourism.

References

1. Shah, M., Akar, F. G., Tomaselli, G. F. Molecular basis of arrhythmias. *Circulation*. **112** (16), 2517-2529 (2005).
2. Bowlby, M. R., Peri, R., Zhang, H., Dunlop, J. hERG (KCNH2 or Kv11.1) K⁺ channels: screening for cardiac arrhythmia risk. *Current Drug Metabolism*. **9** (9), 965-970 (2008).
3. Priest, B. T., Bell, I. M., Garcia, M. L. Role of hERG potassium channel assays in drug development. *Channels (Austin)*. **2** (2), 87-93 (2008).
4. Fenton, F., Cherry, E., Glass, L. Cardiac arrhythmia. *Scholarpedia*. **3** (7), 1665 (2008).
5. Tisdale, J. E. et al. Drug-induced arrhythmias: A scientific statement from the American Heart Association. *Circulation*. **142** (15), e214-e233 (2020).
6. Kramer, J. et al. MICE models: superior to the HERG model in predicting Torsade de Pointes. *Scientific Reports*. **3**, 2100 (2013).
7. Rampe, D., Roy, M.-L., Dennis, A., Brown, A. M. A mechanism for the proarrhythmic effects of cisapride (Propulsid): high affinity blockade of the human cardiac potassium channel HERG. *FEBS Letters*. **417** (1), 28-32 (1997).
8. Girouard, S. D., Laurita, K. R., Rosenbaum, D. S. Unique properties of cardiac action potentials recorded with voltage-sensitive dyes. *Journal of Cardiovascular Electrophysiology*. **7** (11), 1024-1038 (1996).
9. Herron, T. J., Lee, P., Jalife, J. Optical imaging of voltage and calcium in cardiac cells & tissues. *Circulation Research*. **110** (4), 609-623 (2012).
10. Hou, J. H., Kralj, J. M., Douglass, A. D., Engert, F., Cohen, A. E. Simultaneous mapping of membrane voltage and calcium in zebrafish heart in vivo reveals chamber-specific developmental transitions in ionic currents. *Frontiers in Physiology*. **5**, 344 (2014).
11. Ronzhina, M. et al. Di-4-ANEPPS modulates electrical activity and progress of myocardial ischemia in rabbit isolated heart. *Frontiers in Physiology*. **12**, 1-15 (2021).
12. Beck, C., Gong, Y. A high-speed, bright, red fluorescent voltage sensor to detect neural activity. *Scientific Reports*. **9** (1), 15878 (2019).
13. Blinova, K. et al. International multisite study of human-induced pluripotent stem cell-derived cardiomyocytes for drug proarrhythmic potential assessment. *Cell Reports*. **24** (13), 3582-3592 (2018).
14. Kovacs, G. T. A. Electronic sensors with living cellular components. *Proceedings of the IEEE*. **91** (6), 915-929 (2003).
15. Tertoolen, L. G. J., Braam, S. R., van Meer, B. J., Passier, R., Mummery, C. L. Interpretation of field potentials measured on a multi electrode array in pharmacological toxicity screening on primary and human pluripotent stem cell-derived cardiomyocytes. *Biochemical and Biophysical Research Communication*. **497** (4), 1135-1141 (2018).
16. Deo, M., Akwaboah, A., Tsevi, B., Treat, J. A., Cordeiro, J. M. Role of the rapid delayed rectifier K⁺ current in human induced pluripotent stem cells derived

- cardiomyocytes. *Archives of Stem Cell and Therapy*. **1** (1), 14-18 (2020).
17. Hondeghem, L. M., Hoffmann, P. Blinded test in isolated female rabbit heart reliably identifies action potential duration prolongation and proarrhythmic drugs: importance of triangulation, reverse use dependence, and instability. *Journal of Cardiovascular Pharmacology*. **41** (1), 14-24 (2003).
 18. Dipalo, M. et al. Intracellular action potential recordings from cardiomyocytes by ultrafast pulsed laser irradiation of fuzzy graphene microelectrodes. *Science Advances*. **7** (15), eabd5175 (2021).
 19. R Core Team. *R: A language and environment for statistical computing: R Foundation for Statistical Computing*. Vienna Austria. <https://www.r-project.org/> (2021).
 20. Wickham, H.. *ggplot2: Elegant graphics for data analysis*. Springer-Verlag New York (2009).
 21. Wickham, H., Girlich, M. *tidyr: Tidy messy data: R package version 1.2.0*. <https://tidyr.tidyverse.org> (2022).
 22. Wickham, H., François, R., Henry, L., Müller, K. *dplyr: A grammar of data manipulation. R package version 1.0.6*. <https://dplyr.tidyverse.org> (2021).
 23. Godfraind, T. Discovery and development of calcium channel blockers. *Frontiers in Pharmacology*. **8**, 286 (2017).
 24. Vater, W. et al. Pharmacology of 4-(2'-nitrophenyl)-2,6-dimethyl-1,4-dihydropyridine-3,5-dicarboxylic acid dimethyl ester (Nifedipine, BAY a 1040)]. *Arzneimittelforschung*. **22** (1), 1-14 (1972).
 25. Kim, I., Boyle, K. M., Carroll, J. L. Postnatal development of E-4031-sensitive potassium current in rat carotid chemoreceptor cells. *Journal of Applied Physiology* (1985). **98** (4), 1469-1477 (2005).
 26. Edwards, S. L. et al. A multiwell cardiac μ GMEA platform for action potential recordings from human iPSC-derived cardiomyocyte constructs. *Stem Cell Reports*. **11** (2), 522-536 (2018).
 27. Fendyur, A., Spira, M. E. Toward on-chip, in-cell recordings from cultured cardiomyocytes by arrays of gold mushroom-shaped microelectrodes. *Frontiers in Neuroengineering*. **5**, 21 (2012).
 28. Hayes, H. B. et al. Novel method for action potential measurements from intact cardiac monolayers with multiwell microelectrode array technology. *Scientific Reports*. **9** (1), 11893 (2019).